Investigations on the beam pointing stability of a pulsed optical parametric oscillator

Andreas Fix[1,*] and Christian Stöckl[1,2]

[1]*Deutsches Zentrum für Luft- und Raumfahrt (DLR), Institut für Physik der Atmosphäre, 82234 Oberpfaffenhofen, Germany*

[2]*Currently with: Papierfabrik Louisenthal GmbH, 83703 Gmund am Tegernsee, Germany*

[*]*Andreas.Fix@dlr.de*

Abstract: Although the beam pointing stability of optical parametric oscillators and amplifiers is important for various applications few results on this parameter have been published. Here, we investigate the beam pointing stability of an injection-seeded, nanosecond optical parametric oscillator, compare it to its pump laser, and measure correlations between them. Although correlation between both quantities are found, the beam pointing stability of the OPO is significantly better that the one of its pump. Furthermore, the concept of the Allan variance is applied to analyze the temporal components of the pointing stability.

OCIS codes: (190.4970) Parametric oscillators and amplifiers; (140.3295) Laser beam characterization.

References and links

1. A. Fix, "Tunable light sources for lidar applications," in: *Atmospheric Physics* U. Schumann, ed., Research Topics in Aerospace (Springer, 2012).
2. M. Schellhorn, M. Eichhorn, C. Kieleck, and A. Hirth, "High repetition rate mid-infrared laser source," C. R. Phys. **8**(10), 1151–1161 (2007).
3. EN ISO 11670:2003, *Lasers and Laser-Related Equipment – Test Methods for Laser Beam Parameters – Beam Positional Stability* (ISO, 2003).
4. A. W. Allan, "Statistics of atomic frequency standards," Proc. IEEE **54**(2), 221–230 (1966).
5. A. Fix, C. Büdenbender, M. Wirth, M. Quatrevalet, A. Amediek, C. Kiemle, and G. Ehret, "Optical parametric oscillators and amplifiers for airborne and spaceborne active remote sensing of CO2 and CH4," Proc. SPIE **8182**, 818206, 818206-10 (2011).
6. P. Groß, L. Kleinschmidt, S. Beer, and C. Fallnich, "Beam position stabilization for a confocal multiphoton microscope," Appl. Opt. **50**(28), 5361–5368 (2011).
7. W. J. Riley, *Handbook of Frequency Stability Analysis* NIST Special Publication 1065, (National Institute of Standards and Technology, Boulder, CO, 2008).
8. J. Caron, Y. Durand, J.-L. Bézy, and R. Meynart, "Performance modeling for A-SCOPE: a space-borne lidar measuring atmospheric CO2," Proc. SPIE **7479**, 74790E, 74790E-15 (2009).
9. C. Kiemle, M. Quatrevalet, G. Ehret, A. Amediek, A. Fix, and M. Wirth, "Sensitivity studies for a space-based methane lidar mission," Atmos. Meas. Tech. **4**(10), 2195–2211 (2011).

1. Introduction

The angular drift of a laser beam is of particular concern in applications such as laser-based metrology (from long-distance guiding systems to short-distance scanning microscopes) and laser-based material processing. Also, for light detection and ranging (lidar) the pointing stability of the laser transmitter is of importance since the beam must be kept within the field-of-view of the receiving telescope.

Optical parametric oscillators (OPOs) are increasingly used for such applications [1] due to their unsurpassed tunability. Unfortunately, their beam pointing stability is still inadequately investigated. As a very rare example, Schellhorn et al. [2] measured the beam pointing stability of a mid-IR OPO pumped by a nanosecond Ho:YAG laser at 10-kHz repetition rate. However, detailed parametric analyses of this parameter are missing.

In the context of this work we therefore investigated the beam pointing stability of a nanosecond, injection-seeded OPO and compared it to the pointing stability of its (Nd:YAG) laser pump. Correlations between the pointing of pump and OPO were analyzed by measuring

#185118 - $15.00 USD Received 8 Feb 2013; revised 12 Apr 2013; accepted 16 Apr 2013; published 25 Apr 2013

both quantities at the same time. In order to characterize the beam positional stability we followed the International Standard EN ISO 11670:2003 [3] which provides guidance for the measurement of this quantity. In addition, the concept of the Allan variance [4] was applied to characterize the pointing stability on different time scales.

As a further step, the difference in OPO beam pointing was analyzed when its wavelength is switched between two distinct values by changing the wavelength of its seed laser. Such mode of operation is required for differential absorption lidar [1].

2. Set-up

2.1 Pump laser system

As the pump laser for the OPO a diode-pumped Q-switched Nd:YAG Laser (Model Spitlight DPSS INNOLAS GmbH, Germany) at a repetition frequency of 100 Hz was used. The laser is built in form of a commonly used master-oscillator power-amplifier (MOPA) design. Here, however, only the oscillator radiation was used. Approximately 13 mJ of pump energy were extracted before entering the amplifier and were used to pump the OPO. Single-longitudinal mode operation of the Nd:YAG laser, which is essential for narrowband operation of the OPO, is achieved by injection seeding. The seed source is a commercially available DFB fiber laser at 1064 nm. The cavity length of the oscillator is controlled via the Q-switch build-up time reduction technique.

The beam quality factor M^2 of the Nd:YAG laser was measured to be of the order of 1.7. To pump the OPO, a beam reduction telescope (1:2.6) was inserted into the pump beam.

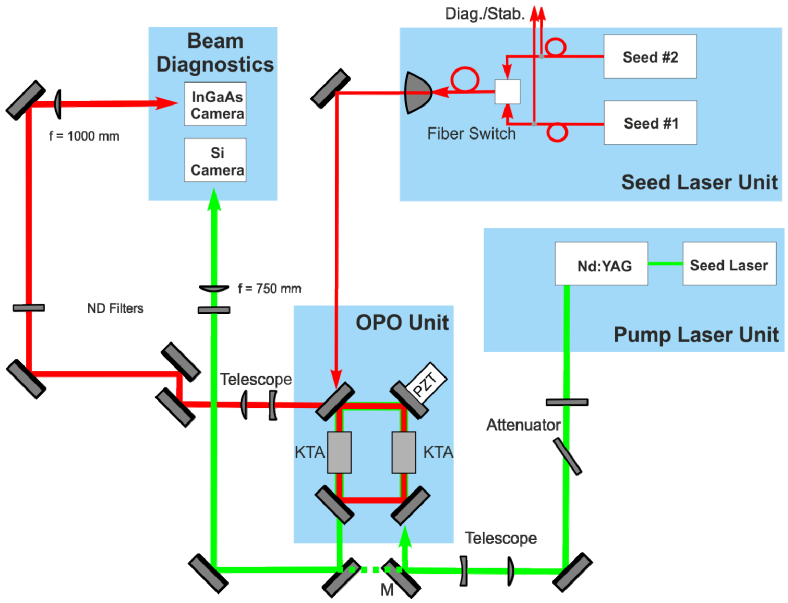

Fig. 1. Schematic set-up of the OPO and the beam diagnostics.

2.2 Optical parametric oscillator

The OPO set-up [5] is designed as a four-mirror ring cavity with potassium titanyl arsenate (KTA) in critical phasematching cut for wavelengths around 1570 nm. The OPO is singly resonant at the signal wavelength and all mirrors were designed for minimum possible reflectivity of the idler wavelength, thus idler radiation present at the entrance apertures of both crystals is negligible. KTA was chosen as the nonlinear optical material since it has much lower absorption in the idler spectral range (~3300 nm) compared to the often used material KTP. Two identical crystals were employed in compensated configuration to partially prevent the walk-off effect. The OPO mirror mounts are attached to a structure

#185118 - $15.00 USD Received 8 Feb 2013; revised 12 Apr 2013; accepted 16 Apr 2013; published 25 Apr 2013

milled from a solid aluminum block. One of the resonator mirrors is attached to a PZT element to match the cavity to the seed wavelength. The whole set-up is depicted in Fig. 1.

Two DFB fiber lasers were used for injection seeding of the OPO. They operate at slightly different wavelengths (on- and off-line) around 1572 nm and are coupled to a fast fiber switch to deliver seed radiation at the selected wavelength to the OPO on a shot-to-shot basis if required. The seed power available for the OPO was of the order of 5 mW. In order to stably seed the OPO, a cavity stabilization technique is necessary to match the cavity length to the seed wavelength. For this purpose, a stabilization concept has been implemented which has been described before [5] and which is based on the measurement of the frequency difference between the outgoing OPO pulse and the incoming cw seed radiation on a shot-by-shot basis using a heterodyne technique. The OPO was operated at ~2 times above OPO threshold with a signal energy of ~2.5 mJ per pulse at 1572 nm. Only the OPO signal beam is used within the context of this work. In order to collimate the OPO beam, a Galilean telescope with a magnification of 2 is used.

2.2 Camera systems

For the position sensing of a laser beam's centroid, there are essentially three types of detectors: lateral-effect photodiodes, quadrant photodiodes and (CCD or CMOS) cameras. There is no strict guideline provided by the International Standard [3] which detector system is to be favored and depends on the application. Here, we chose cameras since those provide simultaneous information about the energy density distribution.

Table 1. Comparison of the camera systems

Parameter	*SMX-150M*	*XS-USB-FPA-320*
Sensor Material	Si	InGaAs
Sensor Type	CMOS 2/3"	CMOS 2/3"
Spectral band [µm]	0.4 - 1.1	0.9 – 1.7
Maximum resolution [pix]	1280 x 1024	320 x 256
Frame rate @ full res. [fps]	27.5	100
Pixel pitch [µm]	6.7	30
Depth [bit]	10	14

The measuring arrangement used for the investigation of the beam pointing stability, consists primarily of two windowless CMOS camera systems. The first one (Sumix SMX-150M) by which the beam profile of the Nd:YAG laser is analyzed is a Si camera while the second one (Xenics XS-USB-FPA-320) is made of InGaAs providing sensitivity at the OPO wavelengths of 1572 nm. Details about the camera systems are given in Table 1. In order to only detect angular displacements, both cameras are located in the focal planes of focusing lenses. The Nd:YAG's laser beam is focused onto the camera's sensor chip by a lens, with a nominal focal length of f = 750 mm. At the measuring wavelength the actual focal length is 762.5 mm. The second lens, used for focusing the OPO beam, has nominal and actual focal lengths of f = 1000 mm and f = 1025.9 mm, respectively. Adequate neutral density filters are used to attenuate the pulse energies before hitting the sensor chips. Both cameras are controlled via USB-port and run in a specially designed LabView program. After proper background correction, the centroid positions are calculated from the energy distribution of Nd:YAG laser and OPO, respectively.

Unless otherwise mentioned the cameras were operated at a fixed frequency of 20 Hz which is well below the maximum frame rate of the Si-camera. Since the pump laser operates at 100 Hz, its trigger signal was down-converted by a factor of 5 to ensure proper timing of the cameras. As a consequence, only every fifth laser pulse is observed.

3. Analysis of beam angular stability

Concerning the determination of the beam pointing stability we generally follow the recommendations of ISO 11670 [3] throughout this Paper.

#185118 - $15.00 USD Received 8 Feb 2013; revised 12 Apr 2013; accepted 16 Apr 2013; published 25 Apr 2013

The positional movement of the beams' centroids in the focal plane is measured relatively to the laboratory axis system (x,y,z) and divided by the respective focal lengths to yield the angular movement of the beam. The values of the beam angular stability in $\delta\alpha_x$, $\delta\alpha_y$ are defined to be twice the standard deviation of the measured angular movement. Often, it is helpful to relate the angular stability to the divergence angle of the beam. In this case, the *relative* beam angular stability $\delta\alpha_{rel,x}$, $\delta\alpha_{rel,y}$ is derived which is the beam angular stability divided by the divergence angle. Within the context of this investigation we do not perform a transformation into the beams' coordinate systems (the directions parallel and orthogonal to the axis of maximum movement of the asymmetric centroid distribution) in order to better trace down the reasons for drifts and to derive correlations between pump and OPO in the same coordinate frame. The respective beam angular stabilities were derived *including* the telescopes in the respective beam paths. Therefore the absolute stability of the Nd:YAG is a factor of 2 smaller upstream of the telescope whereas it is a factor of 2.6 larger in case of the OPO. We argue that the measured quantities correspond to those for pumping the OPO as well as after recollimating its beam. The relative angular stabilities are anyway not affected by the telescopes.

In general, the ISO standard distinguishes between short-term stability (stability within a time interval of 1 s), medium-term stability (stability within a time interval of 1 min), and long-term stability (stability within a time interval of 1 h). Since any specification shall be made on the basis of a significant number (> 1000) of individual measurements we therefore relinquish to calculate the short-term stability since the nature of the pulsed laser and finite frame rate of the camera prevents to derive 1000 data points within 1 s.

In order to separate short- to medium-term variations from long-term drifts it appears reasonable to apply a technique that has become a standard in frequency measurement: the Allan variance [4]. It was originally developed for the characterization of the frequency stability of precision oscillators, but can be readily extended for the characterization of noise in other physical quantities, as a measure of the precision with which such a physical quantity can be determined after averaging for a given duration. The Allan variance is defined so that its expected value is the same as the standard variance for white frequency-modulated (FM) noise. Recently, Groß et al. [6] have already applied the concept of Allan variance to beam pointing stability.

In the context of this investigation we use the overlapping Allan variance. Overlapping means that the two-sample Allan variance is computed using all combinations of the data set which improves the confidence of the resulting stability estimate [7]. The overlapping Allan variance after $m \cdot \tau_0$ averaging, of an infinite time series y_i of a random variable y with even temporal sampling τ_0 is given by:

$$\sigma_y^2(m \cdot \tau_0) = \frac{1}{2 \cdot m^2 (M - 2m + 1)} \sum_{j=1}^{M-2m+1} \left\{ \sum_{i=j}^{j+m-1} [y_{i+m} - y_i] \right\}^2 \qquad (1)$$

where m is the number of measurements. The Allan standard deviation is the square root of the Allan variance. The most common way to express the time domain stability of a measurement which we also adapt here is by means of sigma-tau plots that show the dependence of stability on averaging time. Log-sigma versus log-tau plots do not only show the dependence of stability but provide means to derive the type of noise since the power law of different noise contributions show specific slopes [7].

4. Results

4.1 Beam pointing stability

The evaluation of the beam pointing stability on a time basis of 1 min of both OPO and Nd:YAG laser revealed that the OPO stability is significantly better than of its pump laser.

On average, using about 10 individual measurements on subsequent days, the beam angular stability of the Nd:YAG laser in the x and y axis was determined to be $\delta\alpha_x = (38.4 \pm$

#185118 - $15.00 USD Received 8 Feb 2013; revised 12 Apr 2013; accepted 16 Apr 2013; published 25 Apr 2013

5.2) µrad and $\delta\alpha_y$ = (35.7 ± 11.0) µrad which is in-line with the specifications given by the manufacturer (< 50 µrad). The beam angular stability of the OPO was (4.7 ± 0.7) µrad in the x direction and (5.1 ± 1.3) µrad in the y direction, respectively. In relation to the divergence of the beams the relative angular beam stability of the OPO is 0.9% whereas the one of the pump laser is approximately 5 times higher. Table 2 gives an overview over the experimental results.

Table 2. Absolute and relative beam angular stability of Nd:YAG pump laser and OPO on a 1-min time scale.

Source	$\delta\alpha_x$ [µrad]	$\delta\alpha_y$ [µrad]	$\delta\alpha_{rel,x}$ [%]	$\delta\alpha_{rel,y}$ [%]
Nd:YAG	38.4 ± 5.2	35.7 ± 11.0	4.7 ± 0.7	4.3 ± 1.2
OPO	4.7 ± 0.7	5.1 ± 1.3	0.9 ± 0.1	0.9 ± 0.2

Also on longer time scales the pointing stability of the OPO is considerably better than of its pump. Figure 2 shows the measurement of the pointing stability of pump beam (left panel) and OPO beam (center panel) as a function of time.

The scatter diagrams of the centroid position were simultaneously recorded over a measurement period of one hour. The beam angular stability derived from this data is 33.9 µrad/28.3 µrad for the pump and 10.2 µrad/8.2 µrad for the OPO in x- /y- directions, respectively. The beam angular stability of the pump was also measured both, by bypassing the OPO (see dashed line in Fig. 1) or by transmitting the beam through the OPO cavity below threshold. Within measurement accuracy no significant differences could be detected in these cases.

These data have been compared to the beam stability of the OPO's seed laser (reflected from the OPO outcoupling mirror) when the OPO was off. The corresponding result is shown in the right panel of Fig. 2. The beam angular stability of the seed during this measurement - which was performed on a different day and lasted only 30 minutes - was 6.7 µrad /4.1 µrad, respectively. We attribute the comparatively high stability of the OPO to the good passive stability of the resonator structure and to an appropriate cavity length much shorter than of the pump.

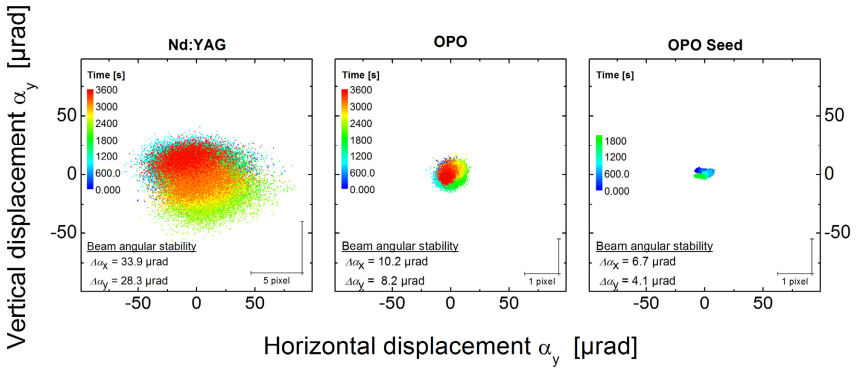

Fig. 2. Record of the beam centroid position for the pump (left panel), OPO (center panel) and OPO seed (right panel) over a time series of one hour (half an hour for the OPO seed). The time (in seconds) is color coded. Nd:YAG pump laser and OPO have been simultaneously recorded, while the pointing of the OPO seed is from a different measurement. All scatter plots are shown in the same scale in units of microradians. The corresponding pixel sizes due to the different cameras are given in the insert scale.

As discussed above, Allan deviations of the beam angular movement on the camera were calculated from this data and are depicted in Fig. 3.

#185118 - $15.00 USD Received 8 Feb 2013; revised 12 Apr 2013; accepted 16 Apr 2013; published 25 Apr 2013

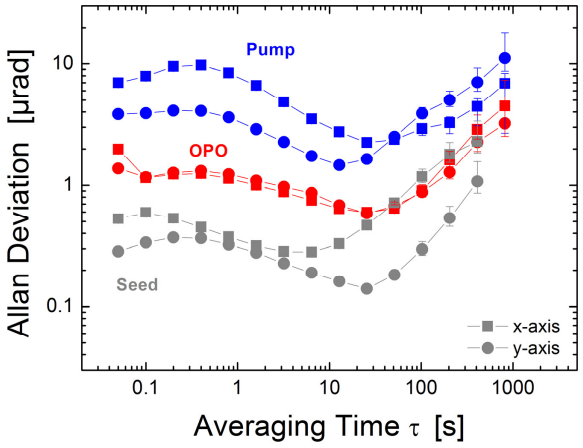

Fig. 3. Sigma-tau plot of the beam angular movement of the pump (blue), OPO (red), and OPO seed (grey) from the measurement of Fig. 2. The squares and circles depict the movement in the x and y-axes, respectively.

This sigma-tau plot shows the Allan deviation of the beam angular movement for the three beams in both x- and y-direction. For averaging times between ~0.5 s to ~10 s white noise is dominating. For averaging times of greater than ~30 s a linear drift becomes obvious for all measurements which we attribute to thermal drifts of the mechanical mounts for beam steering. No special means to stabilize the temperature in the lab have been performed.

4.2 Correlations between pump and OPO

It is now interesting to analyze to what extent the beam pointing of the pump influences the one of the OPO. Therefore we evaluated correlations between their centroid movements in the x and y-axes, respectively. Over a short measurement time of a few hundreds of laser pulses we could not identify a clear correlation. Only if the time series of the centroids were de-trended and averaged with a floating average of 20 seconds some correlation becomes noticeable. This is shown in Fig. 4.

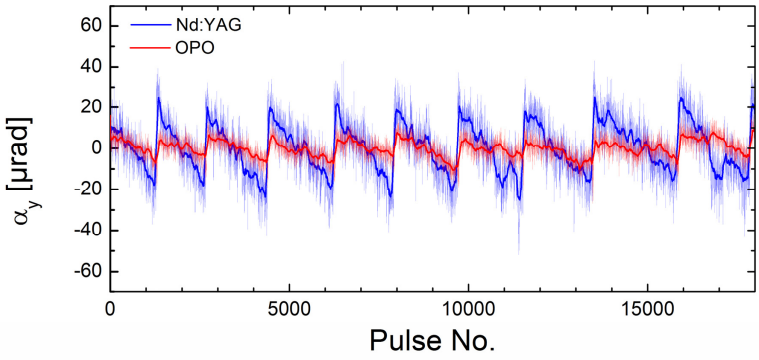

Fig. 4. Time series over 15 minutes of the vertical centroid movement of Nd:YAG laser and OPO, respectively. The data have been de-trended and the thick lines represent a 100-pulse floating average.

With this type of data manipulation a saw-tooth waveform of the vertical centroid movement of the Nd:YAG laser appears. The movement in the horizontal plane also shows this kind of behavior though much less pronounced. To some minor extent the OPO follows this behavior.

#185118 - $15.00 USD Received 8 Feb 2013; revised 12 Apr 2013; accepted 16 Apr 2013; published 25 Apr 2013

The reason for the saw-tooth distortion could unequivocally be attributed to the piezo inside the Nd:YAG resonator that obviously shows a tilt effect. The piezo is automatically reset every few minutes when the Q-switch build-up time stabilization drifts towards the end of the voltage range. This reset causes the saw-teeth which disappear totally when the piezo voltage is kept constant.

Clearly, the influence of the pump beam pointing onto the OPO is rather faint. In order to better distinguish this effect from noise, the steering mirror (denoted by M in Fig. 1) was manually actuated during the measurement, either in the horizontal or vertical plane. Doing so, a pump beam deflection much larger than the jitter is introduced.

As an example, Fig. 5 shows a measurement of the movement in the vertical plane for both OPO and Nd:YAG laser centroid. During this time series of ~20 s the vertical locking screw of the mirror mount that holds beam steering mirror M (see Fig. 1) was manually rotated back and forth. There is a clear correlation between Nd:YAG laser and OPO, but the response of the OPO is damped: the vertical scale for the OPO in Fig. 5 is zoomed in with a factor of 25. Similar results were obtained when the horizontal locking screw steering mirror was actuated.

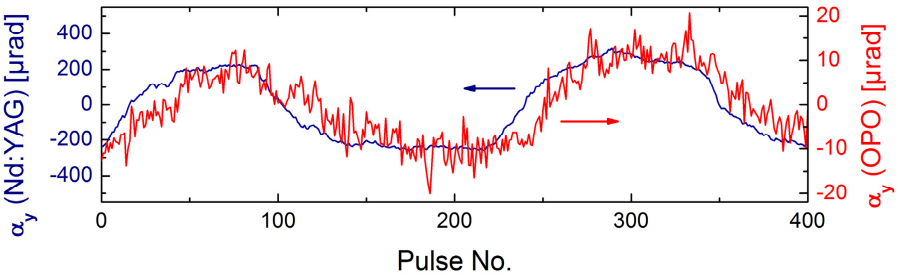

Fig. 5. Time series over 400 pulses of the vertical centroid movement of Nd:YAG laser and OPO, respectively. During this measurement the Nd:YAG laser beam was manually moved in the vertical plane. Note that the right scale is zoomed by a factor of 25.

Figure 6 shows the correlation diagrams between Nd:YAG laser and OPO pointing for horizontal (left panel) and vertical (right panel) motion of the Nd:YAG laser beam. The correlation coefficients were derived to be 0.78 and 0.83 in the horizontal and vertical plane, respectively. Due to the fact that the mirror mount was not gimbaled also some cross correlation between the axes was noticed, which, however, was much smaller. The slopes were calculated to be 1:19 and 1:29 in the horizontal and vertical plane, respectively, which demonstrates the relatively weak direct influence of the Nd:YAG laser pointing onto the OPO pointing. The weak influence is attributed to the fact that the direction of parametric gain is not only determined by the direction of the pump but also by the resonance condition of the cavity.

#185118 - $15.00 USD Received 8 Feb 2013; revised 12 Apr 2013; accepted 16 Apr 2013; published 25 Apr 2013

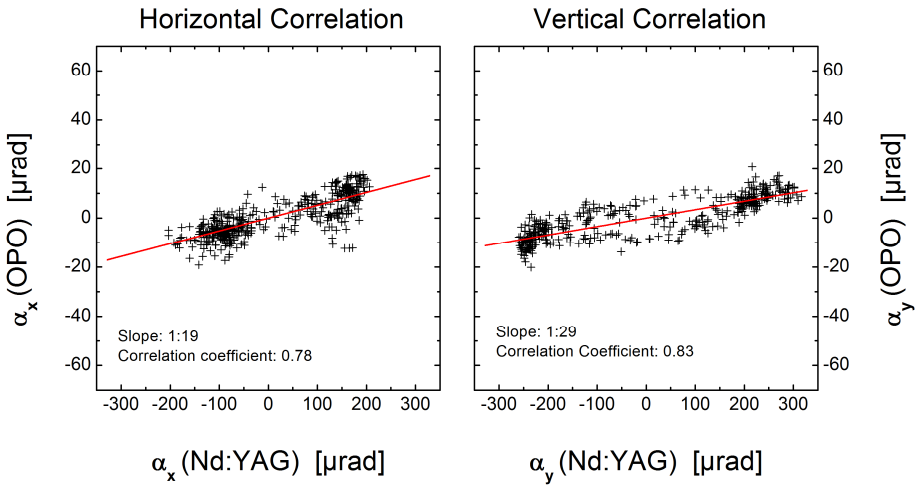

Fig. 6. Dependence of the OPOs beam centroid movement as function of the Nd:YAG laser beam variation. Left panel: The Nd:YAG laser beam is actuated in the horizontal plane. Right panel: The Nd:YAG laser beam is actuated in the vertical plane. Note the different scales for Nd:YAG and OPO angular position.

4.3 Differences between on- and off-line operation

Finally it was to be analyzed whether there is a difference in pointing when the OPO is seeded at different wavelengths as will be the case in a typical differential absorption lidar measurement. Arbitrarily two wavelengths at λ_1 = 1572.012 nm and λ_2 = 1571.893 nm were chosen, which were measured using a wavemeter (High Finesse, WS6 IR). Thus the frequency offset between both wavelengths is $\Delta\nu$~14.4 GHz. The wavelengths were alternatively switched to the OPO at its repetition frequency of the OPO, i.e. 100 Hz using a fiber switch (see Fig. 1). As the InGaAs camera is read out at 20-Hz frame rate, every second data acquisition corresponds to the same wavelength. However, which wavelength corresponds to the even and odd records is uncertain because it depends on which wavelength the series has started with.

Figure 7 depicts the centroid distribution of the OPO for a 10-minute measurement when it was alternatively seeded with the two wavelengths. This measurement shows that the beam angular stability of the OPO operating at the two different wavelengths is very comparable. For the blue distribution the angular stabilities in both orthogonal directions are $\delta\alpha_x$ = 5.5 µrad and $\delta\alpha_y$ = 6.4 µrad. For the red distribution the numbers are slightly worse and amount to $\delta\alpha_x$ = 7.0 µrad and $\delta\alpha_y$ = 7.4 µrad, respectively.

These results agree well with the prior findings (e.g. Table 2). However, there is a small but significant offset between the centers of both scatter plots of ~2.9 µrad. In relation to the divergence of the OPO beam it is of the order of 0.5%, only. This offset may have several reasons. Firstly, since the difference between the two wavelengths was such that it did not coincide with an even multiple of the OPO cavity mode spacing, the active stabilization of the OPO cavity resulted in a different piezo voltage for both wavelengths. A tilt in the piezo's movement may lead to a different beam pointing in a similar way like the piezo in the Nd:YAG laser (compare to Fig. 4). Secondly, the beam profiles for operation of the two different wavelengths could be slightly different so that the centroid location algorithm results in an offset. And thirdly, lateral chromatic aberrations could have occurred in case the light was obliquely incident on the (telescope and focusing) lenses.

#185118 - $15.00 USD Received 8 Feb 2013; revised 12 Apr 2013; accepted 16 Apr 2013; published 25 Apr 2013

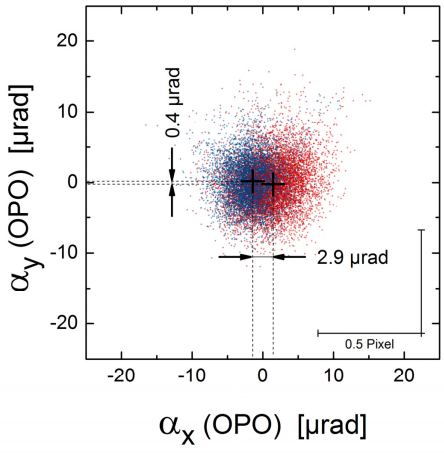

Fig. 7. Centroid distribution for the measurement (10min) of the OPO's pointing stability. The OPO was alternately seeded at two different wavelengths which are color-coded in red and blue.

In order to test the first hypothesis, the OPO was operated with one seed wavelength, only, but the data were analyzed as if two different wavelengths were present. Two separate measurements were performed. In the first series, subsequent pulses were seeded into the same OPO cavity mode, but in the second series the cavity length was alternately changed from pulse to pulse so that the mode number difference for subsequent pulses was 2. The cavity mode spacing is ~2.3 GHz. The results are depicted in Fig. 8.

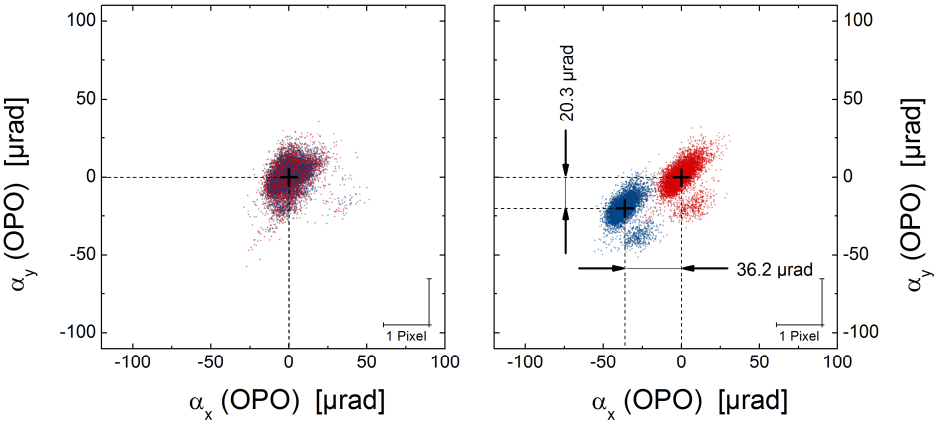

Fig. 8. Centroid distribution for the measurement (10min) of the OPO's pointing stability. Odd and even pulses are color-coded in red and blue. Left panel: The seed is injected into the same longitudinal mode of the OPO resonator. Right panel: the cavity lengths for the "blue" and "red" pulses are two longitudinal mode distances apart.

While the first measurement does not show an offset between the two groups, there is an obvious offset in the second measurement. This is a clear sign that the piezo inside the OPO cavity shows some tilt effect. In order to keep the movement of the piezo as small as possible, a similar measurement as the one depicted in Fig. 7 was repeated, but this time the OPO cavity length was actively matched to the first seed wavelength while the second seed

#185118 - $15.00 USD Received 8 Feb 2013; revised 12 Apr 2013; accepted 16 Apr 2013; published 25 Apr 2013

wavelength was tuned (at a frequency offset of ~11.4 GHz) such that it fitted to the OPO cavity. The result of this measurement is shown in Fig. 9.

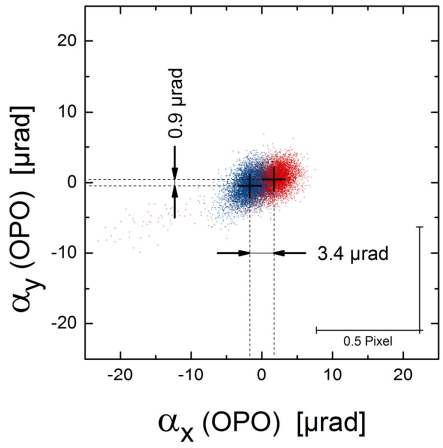

Fig. 9. Centroid distribution for the measurement (10min) of the OPO's pointing stability. The OPO was alternately seeded at two different wavelengths which are color-coded in red and blue. The OPO was actively matched to the first seed wavelength while the second seed wavelength was tuned to match the OPO cavity.

Again, a small offset (3.5 µrad) between the centers of both scatter plots is observed, which is not significantly different from the case where the seed is not matched to the OPO mode (Fig. 7) which means that although there is a tilt effect for substantial changes of piezo voltage some minor offset remains even in case of no difference in mean piezo elongation. Whether this effect is due to a different beam profile or lateral chromatic aberration cannot conclusively be worked out. However, this effect takes place on a scale of less than a per cent of the OPO's beam divergence; hence it is negligible for most applications.

5. Summary and conclusions

The beam pointing fluctuations of a pulsed, injection-seeded OPO were analyzed in detail. The OPO signal beam pointing on a time scale from seconds to hours was measured and compared to the pump laser. For the specific set-up it was shown that the pointing stability of the OPO was significantly (x 5) better than that of its pump. It was demonstrated that beam variations of the pump affect the OPO pointing to a much lesser degree. This means that a good beam pointing stability of an OPO does not necessarily make high demands on the pointing stability of the pump laser. Finally it was also shown that a dual wavelength operation of the OPO which is required for differential lidar applications does not introduce a significant difference in beam pointing. While the beam pointing stability was comparable for both wavelengths a small offset in the beam pointing direction was measured. However, this effect was less than a per cent of the OPO signal divergence and thus appears to be negligible for most applications.

However, the tilt effect of piezo elements inside the pump laser or OPO cavity that are mandatory for single-frequency operation may become an issue and should be avoided for optimum beam stability.

The results of this study are particular suited to help designing future spaceborne lidar transmitters [8,9] and in particular the MERLIN instrument, a spaceborne lidar to measure the important greenhouse gas methane which will be based on an OPO transmitter at a wavelength of 1645 nm. The MERLIN mission is a joint French-German initiative led by the two country's space agencies (CNES and DLR). Its launch is foreseen in the 2016 timeframe.

#185118 - $15.00 USD Received 8 Feb 2013; revised 12 Apr 2013; accepted 16 Apr 2013; published 25 Apr 2013

Acknowledgments

This work was performed on behalf of DLR Space Administration through Astrium GmbH with support from the German Federal Ministry of Economics and Technology under grant FKZ 50 EP 1001. The responsibilities for the content of this publication are those of the authors.

#185118 - $15.00 USD Received 8 Feb 2013; revised 12 Apr 2013; accepted 16 Apr 2013; published 25 Apr 2013